

Chemical and mechanical analysis of tribofilms formed from fully formulated oils Part 2 – Films on Al–Si alloy (A383)

G. Pereira^{*1}, A. Lachenwitzer¹, Y. R. Li¹, M. Kasrai¹, G. M. Bancroft¹,
P. R. Norton¹, M. Abrecht², P. U. P. A. Gilbert^{2,3}, T. Regier⁴, Y. F. Hu⁴ and
L. Zuin⁴

The interactions of a commercially available fully formulated oil on an Al–Si alloy have been studied, and a chemical and mechanical characterisation of the resulting surface films has been undertaken to compare with the results found on 52100 steel. ZnS and Ca phosphate are the primary species found. No Mo species were found in the film, but B was detected; the latter observation contrasts with the results found for 52100 steel. A surprisingly consistent indentation modulus was found for the films formed on A383, considering the complex microstructure of the alloy, which has been shown previously to influence the mechanical response of the film produced from zinc dialkyl dithiophosphates (ZDDPs) in oil. The stiffness of the films on A383 is statistically indistinguishable from that found on 52100 steel, and the topography of the film also looks unchanged compared to the steel study.

Keywords: Fully formulated oils, A383, XANES, Mechanical properties, Antiwear film, Tribofilm

Introduction

Al–Si alloys constitute a class of material that is being used to replace cast iron components in automobile engines. Benefits of the replacement to the car industries include reduction in weight, resistance to corrosion, good thermal conductivity and moderate costs. Al is alloyed with Si to increase the strength of the material and it is well known that Si solidifies in a separate hard phase, which becomes the load bearing surface.

The first cylinder block with an Al–Si liner was used by General Motors (GM) in the Chevrolet Vega engine.^{1,2} The bore was electrochemically etched to expose the primary Si grains on the surface. Experience showed that bores that were not etched resulted in cold scuff failures, and when over etched, resulted in high piston wear and ring wear, most likely due to over exposure of the Si grains that become dislodged in the etching process, generating many hard third bodies.² The Chevrolet Vega was discontinued at the end of the 1977 model year, and GM resorted back to cast iron. However, the motivation to reduce vehicle weight and

increasingly restrictive environmental legislation, has led to Al–Si alloys being considered again to replace cast iron and steel in engines.

Much previous work has focused on the dry sliding of Al–Si alloys,^{3–6} and very little on the lubrication of these alloys.^{7–11} It is well known that the steel/Al couple is a difficult system to lubricate even at modest loads,^{7,10} and furthermore that additives added to formulated oils protect steel, cast iron and Al–Si alloy surfaces, do so by forming protective films.^{12,13} These studies have previously focused on films formed from only ZDDPs diluted in base oils. The novelty of the present paper and the preceding paper is the characterisation of the films formed from fully formulated oils (FF oils).

Part 1 of the present study¹⁴ focused on the interaction of fully formulated oils with steel and the resulting chemistry, morphology and mechanical properties of the antiwear films formed. In the present paper (Part 2), the authors will report on the behaviour of the same oil with an A383 Al–Si alloy and contrast the properties of the two systems.

Experimental

Materials, composition of substrate and sample preparation

Cylinder bores of the Al alloy, A383¹⁵ (~0.10%Mg, ~0.15%Sn, ~0.30%Ni, ~0.50%Mn, ~1.3%Fe, ~2.5%Cu, ~3.0%Zn, ~10.5%Si) were prepared at the GM Research and Development Foundry (Warren, MI) and were cut with a wire electric discharge machine

¹Department of Chemistry, University of Western Ontario, London, Ontario, N6A 5B7, Canada

²Synchrotron Radiation Center, University of Wisconsin, Stoughton, WI 53589, USA

³Physics Department, University of Wisconsin at Madison, Madison, WI 53706, USA

⁴Canadian Light Source Inc., University of Saskatchewan, 101 Perimeter Road, Saskatoon, SK., S7N 0X4 Canada

*Corresponding author, email pereiragavin@gmail.com

(EDM) into square discs with dimensions of $12 \times 12 \times 4$ mm (± 0.5 mm). The discs were mechanically polished with 600 and 1200 grit SiC paper and subsequently polished with 0.6, 0.3 and finally 0.05 μm alumina pastes ($R_a \sim 24$ nm, $R_{RMS} \sim 43$ nm). The discs were then washed in methanol in an ultrasonic bath and stored in air to dry.

Model compounds, antiwear film preparation and coefficient of friction

Antiwear films were made on the polished, A383 discs in a Plint high frequency wear tester. The commercial fully formulated oil was Mobil 1 5W-30 and used as is. The elemental metal composition and preferred functionality of the Mobil 1 5W-30 (FF oil) is shown in Table 1 in Part 1.

The coupons and 52 100 steel cylindrical pins (11 mm in length, 6 mm in diameter) were cleaned in an ultrasonic bath using a light hydrocarbon solvent, and then placed in the Plint high frequency wear tester. The FF oil was poured into the Plint wear tester and the steel pin was laid flat against the disc.

A 40 N load was applied to the pin for the A383 samples, compared to the 220 N load used for the steel study (final contact pressure using a 40 N load was between 92–250 MPa, comparable to the steel results found in Part 1). The temperature was raised to the desired value and maintained throughout the experiment, and the pin was reciprocated with a stroke length of 7 mm at a frequency of 25 Hz (0.35 m s^{-1}). The software monitored the lateral force F_T throughout the experiment through the use of a strain gauge, allowing for a calculation of the coefficient of friction μ . The conditions tested with the FF oil are presented in Table 1 (tribofilms are named as in Part 1). After each experiment, excess oil was removed from the discs using tissue paper and then the samples were rinsed in hexane.

Synchrotron radiation studies

Synchrotron radiation studies were carried out at the Canadian Synchrotron Radiation Facility (CSRF) at Stoughton, WI, USA and at the Canadian Light Source (CLS) at the University of Saskatchewan, Saskatoon, Canada.

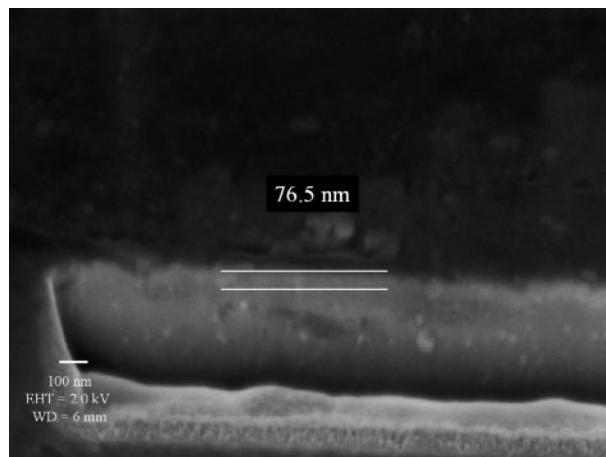
The specifics of the experimental procedure appear in Part 1.

Supplementary XANES data were obtained at the CLS Inc., affiliated with the University of Saskatchewan, Saskatoon.

Some P L-edge data were acquired on the variable line spacing plane grating monochromator beamline covering an energy range of 5.5–250 eV, with a nominal resolution of $\Delta E/E$ better than 1×10^{-4} .

Table 1 Physical parameters tested with FF oil

Time, min	Temp., °C	
5	100	Tribofilm F
30	100	Tribofilm G
720	100	Tribofilm H
30	60	Tribofilm I
30	150	Tribofilm J



1 Tilt corrected SEM (electron yield mode) observation of FIB cross-section of tribofilm G formed on A383: SEM acquired at 2.0 kV and 6 mm working distance; edge of trench is shown on left side of image

Results and discussion

Chemical analysis

Phosphorus

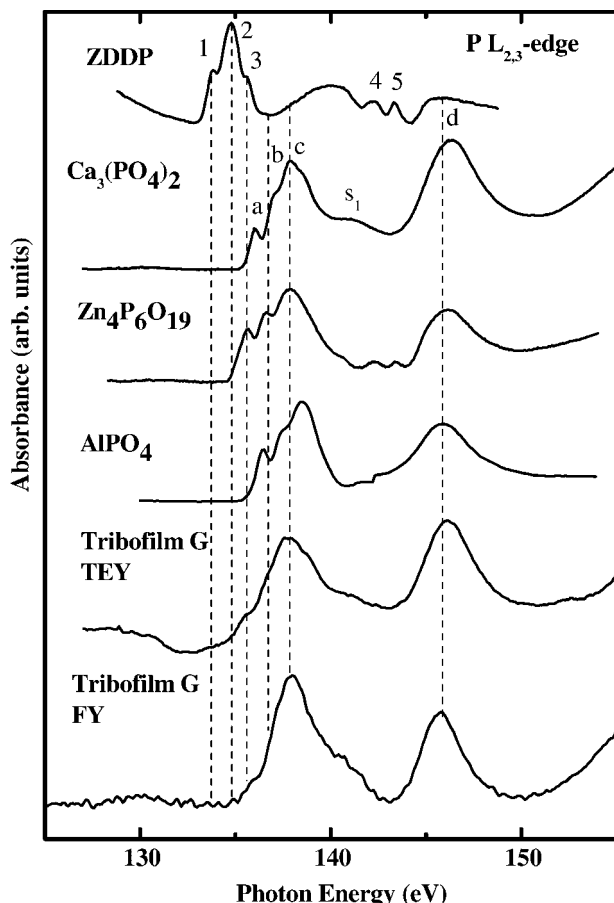
The P K-edge total electron yield (TEY) spectra are very similar to these for the 52100 steel, indicating Ca phosphate as the main product with perhaps some Zn phosphate.

We determined the average P concentration for tribofilms in the same manner as in Part 1. Owing to a very weak FY signal, the P concentration was determined to be very small (1.3×10^{16} atom cm^{-2}). This indicates that the films formed on A383 are slightly less concentrated than those formed on steel and those seen previously from ZDDP (<17 nm assuming a uniform $\text{Zn}_2\text{P}_2\text{O}_7$ film composition). The authors have made cross-sectional cuts in several arbitrary locations using a focused ion beam (FIB) to mill the film. An example of a tilt corrected FIB cross-sectional trench observed through SEM is shown in Fig. 1. The film thickness was found to range between 60 and 80 nm which is thinner than the films formed on steel (Part 1).

Deconvolution of the P K-edge XANES has been previously carried out^{11,16} to estimate the amount of phosphorus species present as either unreacted ZDDP or polyphosphate and the procedure can be viewed elsewhere.⁷ The results of this method indicate that $<5\%$ of the P content remains as unreacted ZDDP with the rest being transformed to polyphosphate, similar to the results obtained on the steel surface (Part 1).

The P L-edge XANES data are shown in Fig. 2. The origins of peaks are already described in Part 1 of this study. A representative spectrum (tribofilm G) for all the tribofilms discussed is shown, collected in both TEY and FY mode and compared to several model compounds. The shoulder s_1 indicates a Ca phosphate, confirming the P K-edge results and those obtained in Part 1.

The FY spectrum shows almost no intensity of peak 2, when compared to the TEY spectrum. This indicates that more unreacted ZDDP is present in the near surface region, and almost none in the bulk of the film consistent with previously obtained results.^{17,18} All acquired spectra were consistent with a polyphosphate structure, but the chain length of the bulk and near surface are



2 P L-edge XANES of tribofilm G: TEY spectrum was acquired at CSRFB grasshopper beamline, and FY was obtained at plane grating monochromator beamline situated at CLS (see text for details)

different. As discussed in Part 1, the ratio of peak 'a' to peak 'c' can yield information about the chain length. The bulk of the film is comprised of polyphosphate of a shorter chain length than the surface region, as evidenced by the less intense 'peak 2' in the FY spectrum. This is evident for all the films made on A383.

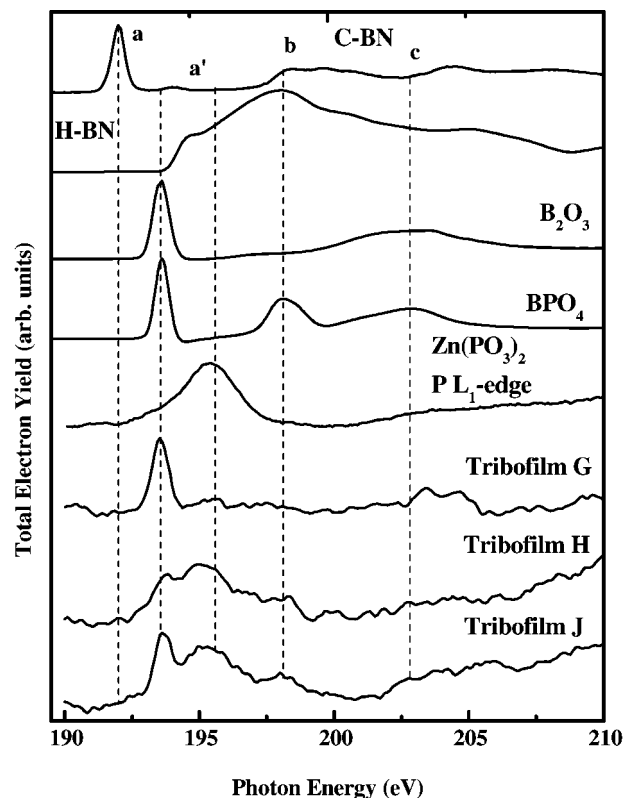
Molybdenum

No Mo L_3 -edge XANES spectrum could be obtained for the film in either the TEY or FY mode for any tribofilms formed on A383.

The authors attempted to make films at 220 N to test if the original 40 N load was not producing high enough contact pressures to form MoS_2 or Mo oxide compounds. However, similar spectra were obtained leading the authors to believe that no Mo containing compounds were incorporated into the tribofilm.

Boron

An brief introduction to boron chemistry is discussed in Part 1, and given in further detail elsewhere.¹⁹ Figure 3 shows the B K-edge spectra (TEY mode) of tribofilms and model boron compounds. In contrast to the results obtained on steel, boron is incorporated into the tribofilm under all the conditions with the exception of the film formed under the longest rubbing time (tribofilm H), which shows only a weak boron signal. The remaining tribofilms show similar spectra to that of tribofilm G. The main peak aligns nicely with that of B_2O_3 .



3 B K-edge XANES of select tribofilms

Calcium, carbon, oxygen and sulphur

The calcium and carbon spectra are very similar to those shown in Part 1. Calcium shows two intense peaks which are the L_3 and L_2 edges. The spectra do not indicate new chemistry, but the data confirm the significant concentration of calcium incorporated into the film.

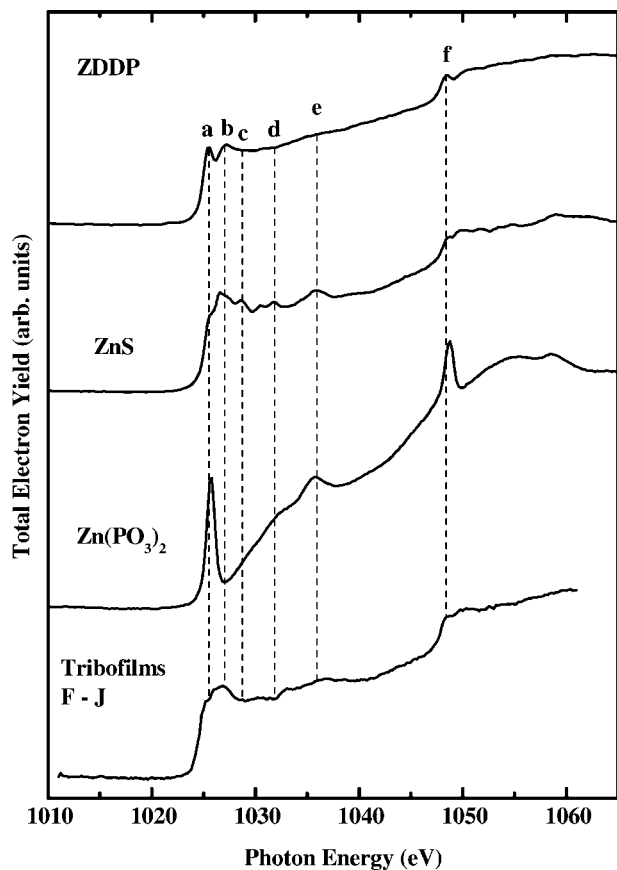
The carbon K-edge XANES collected in FY is similar to that shown in Fig. 7 in Part 1. The TEY collection mode yielded similar results to the FY. A weak peak which corresponds to carbonate, is present in the spectra of the tribofilms. It is difficult to determine the chemistry of carbon, since there are many potential sources such as the oil (hydrocarbon base oil), ZDDP (alkyl groups), detergents and salicylates, not to mention the optics of the beamline. However based on the position of the carbonate peak, some Ca carbonate is deposited in the film, which usually occurs only at high concentration of the detergent and a high degree of overbasing.²⁰

The oxygen spectra are very similar to those shown in Part 1, and will not be further discussed, except it should be pointed out that Al phosphates would also lack the pre-edge peak.

The S spectra were found to be consistent with those in Part 1, however no significant MoS_2 intensity was detected, as expected from the Mo L-edge spectra. The film formed at 150°C (tribofilm J) showed the presence of sulphate, while the remaining films (tribofilms F-I) yielded spectra analogous to ZnS .

Zinc

The Zn L-edge spectra collected in TEY mode are shown in Fig. 4. All the model compounds show intense peaks at $\sim 1025.8 \pm 0.5$ eV. Unfortunately, this peak is not very useful for chemical identification of the Zn species. As in Part 1, we do not see evidence for the formation of ZnO (refer to Part 1 for spectra) in either



4 Zn L-edge XANES of representative tribofilm

the TEY or the FY spectra, which is usually believed to be present as a product of the phosphate reactions.²¹ At higher energies, the model compounds have markedly different spectra which enables us to distinguish ZnS from the different phosphates. The rich above edge structure is currently being investigated by density functional theory calculations, but from a qualitative view point, several comments can be made.²²

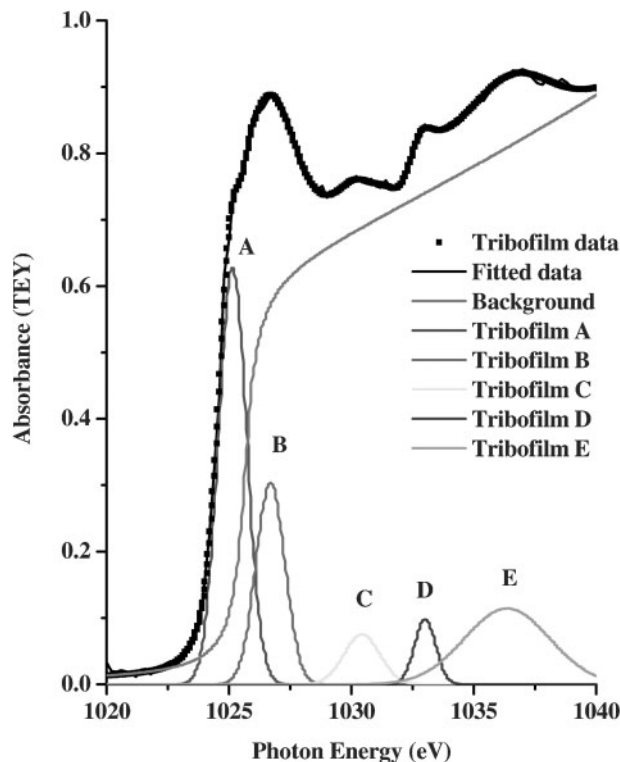
This spectrum looks remarkably different from that found in Part 1. It appears as if the film consists of much more ZnS than found in Part 1.

From Part 1, the deconvoluted peak areas give a semiquantitative ratio of ZnS to zinc phosphate in the wear scar (Fig. 5). All spectra were normalised to peak A, and an arctangent background was subtracted. In total, five peaks were fit (peaks A–E) for ZnS and the tribofilms, and the ratios of integrated heights were compared. Two peaks were fit for zinc phosphates and ZDDP (for details, see Ref. 14). The averaged integrated peak area for ZnS was found to range from $\sim 54 \pm 10\%$ from the normalised peak.

Based on the peak areas of the features beyond the white line, we conservatively estimate the Zn content of the film to be $\geq 85\%$ ZnS (Table 2). However, the alignment of all the satellite peaks are aligned to ZnS,

Table 2 Peak ratios of deconvoluted Zn $2p_{3/2}$ L-edge: peaks are normalised to peak A

	A/A	B/A	C/A	D/A	E/A
ZnS	1	0.55	0.49	0.53	0.61
ZDDP	1	0.37	–	–	–
Tribofilm F–J	1	0.47	0.31	0.24	0.31



5 Normalised and deconvoluted Zn $2p_{3/2}$ edge of representative spectra for tribofilms F–J

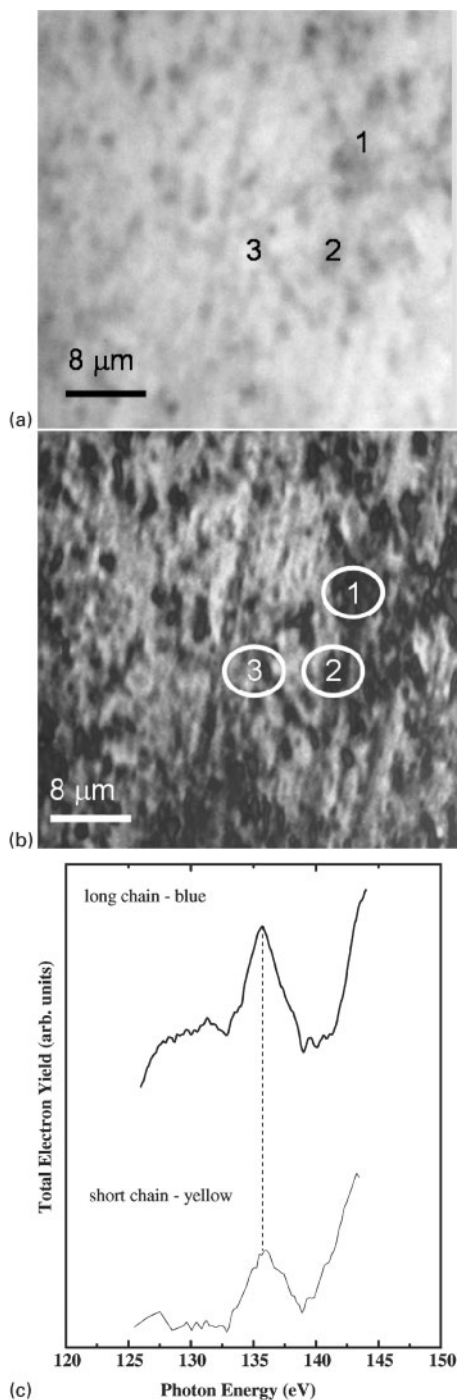
a more plausible estimation is $\geq 90\%$. In films formed from ZDDP in base oil, it was determined that ZnS is only a minor component of the overall film, and the Zn is usually associated with P and not S.²³ This behaviour was also found for the interaction of fully formulated oil with steel (Part 1). In contrast, the results obtained for the Al–Si system show that a large majority of Zn is present as ZnS.

X-PEEM

X-PEEM images were acquired for the FF oil antiwear films. Spectra were generated for P, S, B, Ca, Mo, C, and O.

Figure 6a and b respectively shows the secondary electron X-PEEM image and the phosphorus X-PEEM distribution map of tribofilm G obtained using the internal model spectra shown in Fig. 6c. Details of the X-PEEM analysis can be found elsewhere.^{24–27} Briefly, spectra from pixels or regions of interest in the antiwear film are compared with model spectra for different chain lengths and assigned a colour based upon whether they are characteristic of long or short chain polyphosphates. A linear regression analysis was applied pixel by pixel to the acquired image sequence, from which component maps were generated, and regions corresponding to long (blue) and short (yellow) chain polyphosphate distribution were constructed for tribofilm G (Fig. 6b). Regions whose spectra match quite well to the internal model spectra are coloured while black areas in Fig. 6b indicate the absence of a good fit to either model spectrum. This analysis is only semiquantitative since the films are probably complex mixtures containing a wide range of chain lengths but the images do capture the overall distribution of long and short chain polyphosphates.

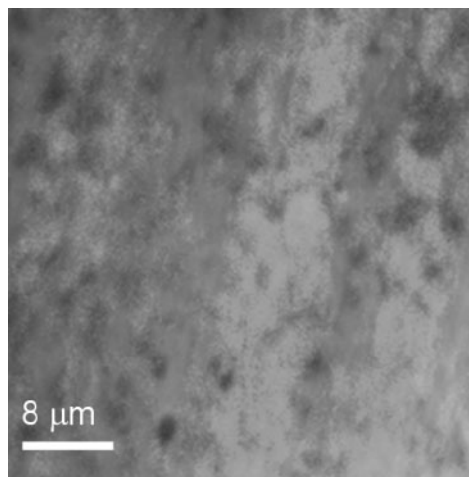
The area analysed in Fig. 6b is primarily comprised of short chain (yellow) polyphosphates ($alc=0.41$), with a



6 Phosphorus X-PEEM for tribofilm G *a* secondary electron image obtained with X-PEEM, *b* distribution map and *c* corresponding spectra: yellow regions indicate short chain polyphosphates and blue areas represent areas of long chain polyphosphates; black areas are regions where spectra did not fit well with either long or short chain polyphosphates; regions of interest are outlined which can be compared to Fig. 8

few locations containing long chain (blue) polyphosphates ($alc=0.56$). See Part 1 for discussion about the interpretation of alc ratios.

Figure 7 is the B X-PEEM distribution map. Boron was collected in second order harmonic due to the limitation of the beamline. The peak which is usually at ~ 192 eV (see Fig. 3) appears at ~ 96 eV collected in second order (not shown). Two regions were found in



7 Boron X-PEEM distribution map for tribofilm G

the area analysed, one with no B signal (magenta areas) and one with a weak B peak (green areas). As one can see from Fig. 7, B is distributed over the region analysed, albeit, regions where no B was measured, appear. This coincides with the rubbing direction.

Unfortunately owing to the poor S/N, meaningful spectra could not be extracted for the Mo L-edge (although none were expected, see section 'Molybdenum'), or the S L-edge. Within the region of interest, no internal chemical differences were found in the spectra of Ca, O or C. As expected, Ca, C and O were evenly distributed across the films.

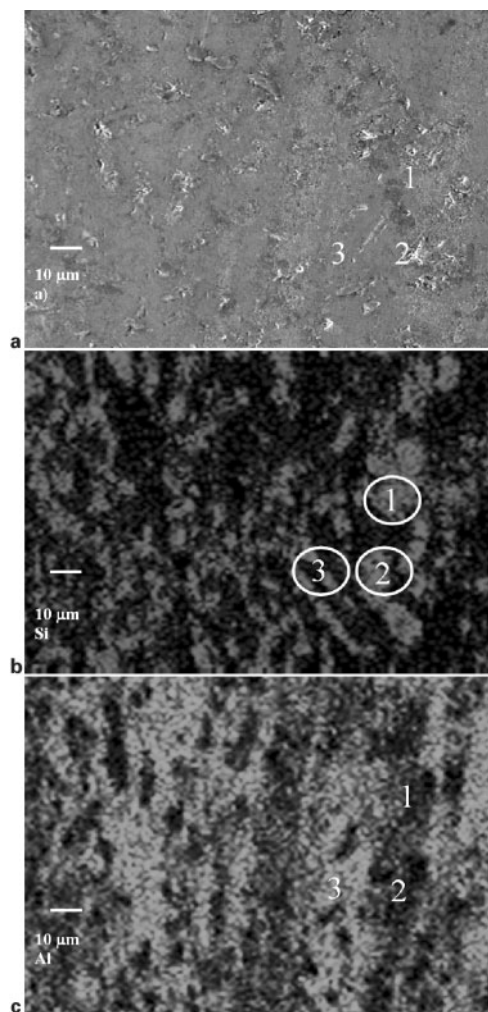
SEM/EDX, AFM and indentation characterisation

Figure 8 shows the mapping SEM/EDX of the regions studied by X-PEEM (Figs. 6 and 7) to identify and attempt to correlate any chemical changes to surface and subsurface components. Figure 8*a* is a 5.0 kV SEM image collected in field emission mode to enhance the surface sensitivity of tribofilm G. Figure 8*b* and *c* are EDX elemental component maps for Si and Al respectively. The brighter areas correspond to an abundance of that particular element.

The authors have previously shown that long chain polyphosphates form exclusively on the Si grains while shorter chained species form on the Al matrix^{11,16} in studies of films formed from ZDDP in oil. A comparison of the images in Figs. 6*b*, 8*b* and *c*, indicate that a similar effect is also observed in the present study, although the distinction between Al rich and Si rich regions is not so distinct. This means that regardless of additive, the longer chain species forms on the Si grain.

Figure 9 is a representative $75 \times 75 \mu\text{m}^2$ AFM height image of the tribofilm G. The film's topography looks very heterogeneous and similar to the FF film formed on steel (Part 1). In the steel work, the topography generated from the FF oil appears continuous with exception of the trenches. No trenches are detected on the Al-Si system, which the authors attribute to the considerable difference in loads used (40 N for the Al-Si experiments v. 220 N in the steel work).

Instrumented nano-indentation was performed on the FF oil samples. Details of the instrumentation, calibration, calculations and assumptions are given elsewhere.^{26,28} Topographic images were taken prior to taking an indent and after indenting a region with the same tip. Force-distance ($f-d$) curves were taken with



8 a field emission 5.0 kV SEM image for tribofilm G and b, c mapping EDX of same region: brighter areas correspond to abundance of that particular element shown; regions of interest are outlined which can be compared to Fig. 6

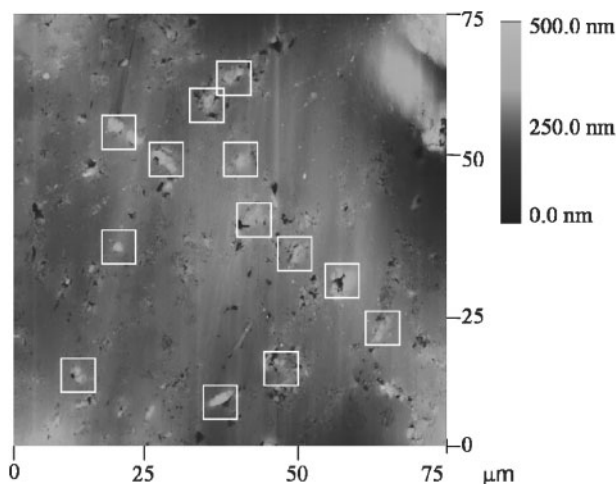
loads of 30 μN for the tribofilms, to minimise the influence of the underlying substrate.

The indentation modulus E_s^* is a commonly used value to compare the film's stiffness without prior knowledge of the material's Poisson's ratio, while taking into account the mechanical influence of the indenting tip. Table 3 evaluates the differing mechanical properties of the FF oil and compares these values to the subcomponents of the substrate.¹⁶

The boxed regions in Fig. 9 were believed to be Si grains in the near surface region, based on the SEM/EDX data. Within statistical error, there does not appear to be any mechanical differences between boxed and non-boxed regions. From the SEM/EDX we know

Table 3 Indentation moduli E_s^* of different locations on tribofilm G (see Fig. 9), presented with other data pertinent for comparison

	Indentation modulus E_s^* , GPa
Al matrix	~ 97
Si grains	~ 193
Boxed regions	108 ± 29
Non-boxed regions	99 ± 30

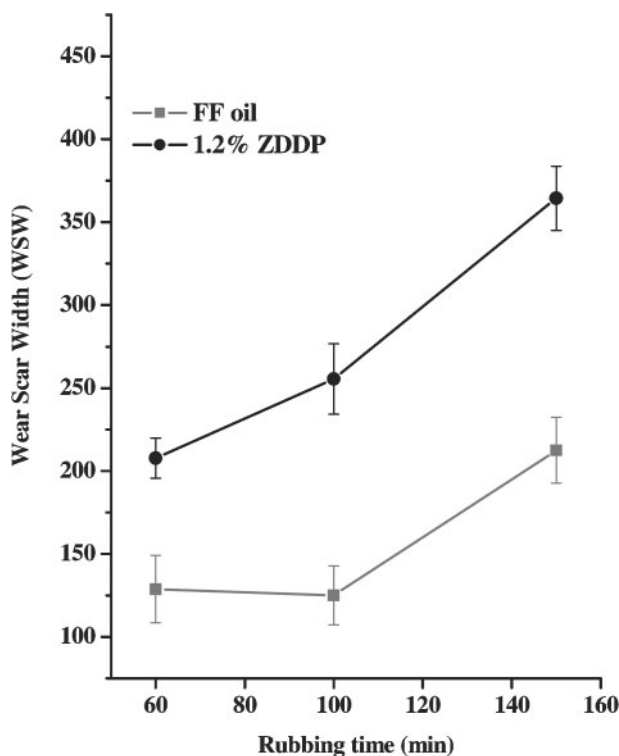


9 Representative contact 75 × 75 μm² AFM image for tribofilm G: this area is same as displayed in Figs. 1, 6 and 9. The boxed regions are believed to be Si grains (see text). The arrow designates rubbing direction

the indenter is sampling the films formed on both the Al matrix and Si grains. The values presented are assumed to be a representative modulus for all the FF tribofilms. It is not possible to determine whether any single additive has a significant influence on the indentation modulus versus the final formulated package. However, the data indicate that the antiwear pads formed on A383 have similar mechanical properties to the FF pads formed on steel (~125 GPa).

Friction coefficient and wear scar width

The averaged μ value (calculated from a normal force F_N of 40 N) taken from all the FF oil samples, was found to be 0.11 ± 0.01 . This is typical for the boundary lubrication regime of ZDDP films.²⁹ The value is similar



10 Wear scar width as function of rubbing temperature

to that obtained for FF oil on steel (Part 1), as well as to those previously reported in studies involving the A383 alloy.¹⁶

The wear scar widths as a function of rubbing temperature for the films formed from FF oils are compared to previous results from ZDDP only (from Ref. 16 and unpublished results) and are given in Fig. 10. The findings are once again contradictory to the results found on steel (where the wear was found to increase comparing FF oil to ZDDP itself), by showing a significant decrease in wear for the FF oil. These findings are consistent with our dual additive study,³⁰ where the improved wear behaviour was attributed to the presence of a phenate. In the dual additive study, MoDTC + ZDDP also showed reduced the wear. This cannot explain the results in the present study, since no Mo species were detected. Furthermore, we have previously attributed the decreased wear to the increased film thickness, and from the present study we do not have evidence for thicker films (indirectly related to P concentration & FIB milling).

Conclusions

In Part 2 of the present study, the authors report on the investigation of the chemical and mechanical properties of tribofilms formed from FF oils on an Al-Si alloy (A383). The following conclusions can be made.

1. Medium chain Ca polyphosphate film is formed.
2. No molybdenum was found in the film, while evidence of B was found; the reverse behaviour was found on 52100 steel (Part 1).
3. The chemistry of Ca, O, S and C (CO_3^{2-}) was found to be similar to the work on steel (Part 1).
4. Approximately 85% of the film was found to be ZnS, while ~15% was found to be unreacted ZDDP and Zn phosphate.
5. B K- and P L-edge X-PEEM distribution maps were generated, and compared to SEM/EDX maps. Longer chain polyphosphate was correlated with the Si.
6. The mechanical properties of the film formed on the Si grains and Al matrix regions appeared to be identical. This contrasts with the behaviour observed on A383 rubbed in a lubricant of ZDDP in base oil.
7. One of the most surprising finds was the very low wear found compared to ZDDP alone. This decrease in wear with FF compared to ZDDP contrasts sharply with the increased wear observed on 52100 steel. This might be a very significant observation with respect to identifying lubricant packages which are effective on Al-Si alloys.

Acknowledgements

The authors would like to thank Mr Phil Shaw and Mr Brian Dalrymple of the Physics Machine Shop, Mr Gord Wood of the Earth Sciences Department and Dr Leighton Coatsworth (all from The University of Western Ontario) for useful discussions and technical support. The authors would like to thank Ross Davidson and the staff at Surface Science Western (SSW) for assistance in acquiring the SEM/EDX data and Dr Todd Simpson from the Nanofabrication Laboratory for assistance in acquiring the FIB/SEM

results. The research described in this manuscript was performed partially at the Canadian Light Source, which is supported by NSERC, NRC, CIHR, and the University of Saskatchewan. We are also grateful to Dr Astrid Jürgensen from the Canadian Synchrotron Radiation Facility (CSRFB), University of Wisconsin, Madison, for her technical support, and the National Science Foundation (NSF) for supporting the SRC under grant No. DMR-0537588. This work was financially supported by the Natural Sciences and Engineering Research Council of Canada (NSERC), General Motors of Canada Ltd, General Motors R & D Center and by the National Research Council of Canada (NRC) which supports the Canadian Synchrotron Radiation Facility at the Aladdin ring in Stoughton, Wisconsin.

References

1. L. E. Reuss and C. N. Hughes: *SAE Congr.*, 1971, **710150**, 577.
2. F. J. Kneisler, D. A. Martens and R. W. Midgley: *SAE Congr.*, 1971, **710147**, 520.
3. A. T. Alpas and J. Zhang: *Wear*, 1992, **155**, 83.
4. X. Y. Li and K. N. Tandon: *Wear*, 2000, **245**, 148.
5. Z. Ma, J. Bi, Y. Lu, H. Shen and Y. Gao: *Wear*, 1991, **148**, 287.
6. P. B. N. Bai and S. K. Biswas: *ASLE Trans.*, 1986, **29**, 116.
7. M. A. Nicholls, P. R. Norton, G. M. Bancroft and M. Kasrai: *Wear*, 2004, **257**, 311.
8. C. M. Chen, C. C. Yang and C. G. Chao: *Mater. Sci. Eng. A*, 2005, **A397**, 178.
9. M. Fuller, M. Kasrai, J. S. Sheasby, G. M. Bancroft, K. Fyfe and K. H. Tan: *Tribol. Lett.*, 1995, **1**, 367.
10. Y. Wan, L. L. Cao and Q. J. Xue: *Tribol. Int.*, 1997, **30**, 767.
11. G. Pereira, A. Lachenwitzer, M. A. Nicholls, M. Kasrai, P. R. Norton and G. De Stasio: *Tribol. Lett.*, 2005, **18**, 411.
12. H. Spikes: *Tribol. Lett.*, 2004, **17**, 469.
13. M. A. Nicholls, T. Do, P. R. Norton, M. Kasrai and G. M. Bancroft: *Tribol. Int.*, 2005, **38**, 15.
14. G. Pereira, A. Lachenwitzer, M. Kasrai, G. M. Bancroft, P. R. Norton, M. Abrecht, P. U. P. A. Gilbert and T. Reiger: *Tribol. Mater. Surf. Interf.* 1 (2007) 1.
15. 'Aluminum alloys'; 1985, Materials Park, OH, ASM International.
16. G. Pereira, A. Lachenwitzer, M. Kasrai, P. R. Norton, T. W. Capehart, T. A. Perry, Y.-T. Cheng, B. Frazer and G. De Stasio: *Tribol. Lett.* 26 (2007) 103.
17. Z. Yin, M. Kasrai, M. Fuller, G. M. Bancroft, K. Fyfe and K. H. Tan: *Wear*, 1997, **202**, 172.
18. M. Suominen-Fuller, M. Kasrai, G. M. Bancroft, Chemical applications synchrotron radiation. In: *Advanced Series in Physical Chemistry: Part 2*, 12B, T. K. Sham (World Scientific Publishing Co., New Jersey, 2002).
19. Z. Zhang, E. S. Yamaguchi, M. Kasrai and G. M. Bancroft: *Tribol. Trans.*, 2004, **47**, 527.
20. Y. Wan, M. L. Suominen Fuller, M. Kasrai, G. M. Bancroft, K. Fyfe, J. R. Torkelson, Y. F. Hu, K. H. Tan, Effects of detergent on the chemistry of tribofilms from ZDDP: Studied by X-ray absorption spectroscopy and XPS. In: *Boundary and Mixed Lubrication: Science and Applications*, 40, D. E. A. Dawson (Elsevier Science B. V., 2002).
21. J. M. Martin: *Tribol. Lett.*, 1999, **6**, 1.
22. G. Pereira, Y. M. Yiu, Y. Li, A. Lachenwitzer, M. Kasrai, G. M. Bancroft, P. R. Norton, T.-K. Sham, T. Regier, R. Blyth, J. Thompson, Y. Hu and L. Zuin: In preparation, 2006.
23. H. Spedding and R. C. Watkins: *Tribol. Int.*, 1982, **99**, 9.
24. G. Pereira, A. Lachenwitzer, M. A. Nicholls, M. Kasrai, P. R. Norton and G. De Stasio: *Tribol. Lett.*, 2004, **18**, 411.
25. M. A. Nicholls, G. M. Bancroft, M. Kasrai, P. R. Norton, B. H. Frazer and G. De Stasio: *Tribol. Lett.*, 2004, **18**, 453.
26. M. A. Nicholls, P. R. Norton, G. M. Bancroft, M. Kasrai, T. Do, B. H. Frazer and G. De Stasio: *Tribol. Lett.*, 2003, **17**, 205.

27. M. A. Nicholls, G. M. Bancroft, P. R. Norton, M. Kasrai, G. De Stasio, B. H. Frazer and L. M. Wiese: *Tribol. Lett.*, 2004, **17**, 245.
28. G. Pereira, D. Munoz-Paniagua, A. Lachenwitzer, M. Kasrai, P. R. Norton, T. W. Capehart, T. A. Perry and Y.-T. Cheng: *Wear*, 2006, **262**, 461.
29. C. Grossiord, J. M. Martin, T. Le Mogne and T. Palermo: *Tribol. Lett.*, 1999, **6**, 171.
30. G. Pereira, A. Lachenwitzer, D. Munoz-Paniagua, M. Kasrai, P. R. Norton, T. W. Capehart, T. A. Perry and Y.-T. Cheng: *Tribol. Mater. Surf. Interf.* 1 (2007) 4.